Nikolaos Biris[1]
Athanassios Stavrakoudis[1]
Anastasia S. Politou[2]
Emmanuel Mikros[3]
Maria Sakarellos-Daitsiotis[1]
Constantinos Sakarellos[1]
Vassilios Tsikaris[1]
[1] *Department of Chemistry, University of Ioannina, 45110 Ioannina, Greece*

[2] *Medical School, University of Ioannina, 45110 Ioannina, Greece*

[3] *Department of Pharmacy, University of Athens, 15771 Athens, Greece*

Received 27 March 2002; accepted 21 October 2002

The Ac–RGD–NH_2 Peptide as a Probe of Slow Conformational Exchange of Short Linear Peptides in DMSO

Abstract: *According to general belief, the conformational information on short linear peptides in solution derived at ambient temperature from NMR spectrometry represents a population-weighted average over all members of an ensemble of rapidly interconverting conformations. Usually the search for discrete conformations is concentrated at low temperatures especially when sharp NMR resonances are detected at room temperature. Using the peptide Ac–RGD–NH_2 (Ac–Arg–Gly–Asp–NH_2, Ac: acetyl) as a model system and following a new approach, we have been able to demonstrate that short linear peptides can adopt discrete conformational states in DMSO-d_6 (DMSO: dimethylsulfoxide) which vary in a way critically dependent on the reconstitution conditions used before their dissolution in DMSO-d_6. The conformers are stabilized by intramolecular hydrogen bonds, which persist at high temperatures and undergo a very slow exchange with their extended structures in the NMR chemical shift time scale. The reported findings provide clear evidence for the occurrence of solvent-induced conformational exchange and point to DMSO as a valuable medium for folding studies of short linear peptides.* © 2003 Wiley Periodicals, Inc. Biopolymers 69: 72–86, 2003

Keywords: *arginine ionic interactions; aspartic acid ionic interactions; fibrinogen inhibitor; hydrogen bonds; NMR; peptide folding; RGD peptide; slow conformational exchange*

Correspondence to: Vassilios Tsikaris; email: btsikari@cc.uoi.gr

Contract grant sponsor: Greek Secretariat of Research and Technology

Biopolymers, Vol. 69, 72–86 (2003)

INTRODUCTION

Information on the favored conformational states of short linear peptides comes mainly from x-ray diffraction, NMR studies in different solvents, and molecular modeling calculations.[1–3] For instance, five different crystal structures for Leu-enkephalin and three for Met-enkephalin, depending on solvent crystallization conditions, have been reported.[4,5] By taking advantage of the solubility of peptides in a number of polar solvents, various solvent-dependent conformational states can be resolved. It is generally accepted that these states are found in very fast conformational exchange. The structures of peptides, especially those derived from NMR, are believed to represent only population-weighted averages over all conformers in a given solvent at ambient temperature. Only slow transitions in the NMR time scale conformational, such as the amide bond *cis–trans* interconversion, have been resolved to date for linear peptides by NMR spectroscopy. To study very rapid processes, such as the folding of peptides and proteins, new methods had to be developed (stopped-flow fluorescence, stopped-flow CD, temperature jump, etc.), which allow the earliest events in folding to be probed.[6,7] Using temperature jump and photodissociation techniques, Eaton et al.[8] have shown that some α-helices are formed in a few nanoseconds, whereas others require microseconds to fold, depending on the particular amino acid sequence. To date, intermediate conformational states between folded and unfolded states in peptides have not been detected.

Some recent studies have indicated that short linear peptides can adopt different conformational states in dimethylsulfoxide (DMSO) solutions depending on the pH value of the aqueous solution they originated from.[9–12] We have also provided experimental evidence by ^{17}O-NMR spectroscopy for slow conformational exchange of Boc–[^{17}O]Tyr(2,6-diClBzl)–OH (Boc: *tert*-butoxycarbonyl; Bzl: benzyl) in DMSO solution.[13] Our conclusion was based on the detection of two, rather than one, ^{17}O resonances for the carboxyl group of the peptide in DMSO, most probably due to the engagement of the carboxyl group in a strong hydrogen-bonding interaction. In $CDCl_3$ solution, on the other hand, a single ^{17}O resonance, resulting from the fast exchange between open and hydrogen bonded states, was observed. The dependence of the peptide conformation on the nature of the reconstitution medium has also been highlighted by the recent work of Boden et al., who studied the three-dimensional (3D) structure of a linear 27-residue peptide in lipid bilayers by Fourier transform infrared (FTIR) absorption.[14] When that peptide was reconstituted from methanol, it adopted a β-strand structure, while in the case of 2,2,2-trifluoroethanol it formed initially an α-helix, which relaxed very slowly (within hours) to an equilibrium state between α-helix and β-sheet.

It appears, therefore, that the nature of the solvent and the conditions employed in the conformational reconstitution might influence the prevalence of a certain peptide conformation.

The work reported here aims to develop a NMR-based strategy that would allow us to identify directly discrete conformational states of short linear peptides, differentiate them from the average one, and gain new insight into their folding process. The tripeptide Ac–RGD–NH_2 (Ac–Arg–Gly–Asp–NH_2, Ac: acetyl) was used as a model compound for our NMR and molecular modeling studies.[15–18] Solutions of this peptide in DMSO-d_6, reconstituted from aqueous solutions at different pH values, were studied by ^{1}H-NMR spectroscopy at several temperatures (in the range 300–355 K). We managed to detect discrete conformational states of the peptide in DMSO-d_6, which vary with the initial pH of the solution, and to show that these states can be in slow exchange depending on the reconstitution conditions. We present here our findings and discuss their implications for peptide folding.

MATERIALS AND METHODS

Reagents and solvents were used without further purification. 2-(1H-benzotriazol-l-yl)-1,1,3,3-tetramethyluronium (TBTU), 1-hydroxybenzotriazole (HOBt), and Boc amino acids were purchased from Neosystem (France); solvents from Labscan Ltd. (Ireland); trifluoroacetic acid (TFA) and diisopropylethylamine (DIEA) from Merk Schuchardt (Germany); and 4-methyl-benzhydrylamine resin (MBHA) resin from Saxon Biochemicals (Hannover, Germany). DMSO-d_6 and tetramethylsilane (TMS) were purchased from Eurisotop (France).

Synthesis of Ac–RGD–NH_2

This was carried out by the stepwise solid-phase procedure on a MBHA resin following the Boc chemistry.[19] Arg was introduced as Boc–Arg(Tos)–OH (Tos: toluene-4-sulfonyl) and Asp as Boc–Asp(OBzl)–OH. Coupling reactions were performed using the molar ratio of amino acid/TBTU/HOBt/DIEA/resin 3/2.9/3/3/1. The αNH_2 group, after cleavage of the Boc protecting group with TFA, was acetylated using an excess of Ac_2O in pyridine (the ratio Ac_2O/—NH_2 group was 30:1). Ac–RGD–NH_2 was cleaved from the resin with anhydrous HF in the presence of phenol and anisole as scavengers. The crude material (yield 80%) was subjected to high performance liquid chromatography

(HPLC) purification (semipreparative reverse-phase C_{18} column) using gradient elution with the following solvents: A, H_2O/0.1% TFA; B, CH_3CN/H_2O/TFA (10/90/0.1). A programmed gradient elution (4 mL/min) was applied (A/B: 90/10–A/B: 75/25), elution time 20 min (yield 60%). The purity of the peptide was checked by analytical HPLC and the correct molecular mass was confirmed by electrospray ionization mass spectroscopy (ESI-MS) (MW calc.: 387.40; found: 387.62).

Synthesis of Ac–RGd–NH_2

This was carried out on a MBHA resin according to Boc chemistry as described above. The purity of the peptide was checked by analytical HPLC and the correct molecular mass was confirmed by ESI-MS.

^{1}H-NMR Experiments

The NMR samples were prepared by dissolving the solid material in H_2O, and adjusting the pH to the desired value with NaOH or HCl. The aqueous solutions were lyophilized, and weighted amounts were dissolved in DMSO-d_6 at concentrations ~5 m*M*. The NMR experiments were performed at 295–355 K on Bruker AMX 400 and Avance 500 spectrometers. The standard correlation spectroscopy (COSY), total COSY (TOCSY), and rotating frame nuclear Overhauser effect spectroscopy (ROESY) Bruker microprograms were used. The TOCSY spectra were recorded using a mixing time of 100 ms. The spectral width in F1 was 5600 Hz. Various ROESY experiments were performed using mixing times of 250 and 350 ms at 300, 305, and 310 K.

The rate constants of rotation about the guanidinium N^{ε}–C^{ζ} (k_{ε}), C^{ζ}–$N^{\eta 1}$ ($k_{\eta 1}$), and C^{ζ}–$N^{\eta 2}$ ($k^{\eta 2}$) bonds were obtained by calculating the NMR line shape for a four-site exchange process using the general multiple site exchange matrix algorithm.[20] The best fitted simulated spectra were obtained by using the spectral parameters (chemical shifts, line widths, and intensities) for guanidinium protons and varying rate constants k_{η}, $k_{\eta 1}$, and $k_{\eta 2}$. The natural line widths of guanidinium NH signals required in these determinations were estimated by measuring the line widths of nonexchanging Arg amide proton signals at appropriate temperatures. All calculations were performed using the program Muses (*MU*ltiple *S*ite *E*xchange *S*imulations).[21] The activation parameters were evaluated from *Eyring* equations:

$$\ln(k/T) = 23.76 - (\Delta H^*/RT) + (\Delta S^*/R)$$

and

$$\Delta G^* = RT[23.76 - \ln(k/T)]$$

where R is the universal gas constant.

Structure Calculation

Structure calculation was carried out using the software DYANA (*DY*namics *A*lgorithm *N*MR *A*pplications).[22] The distance restraints used as inputs in DYANA were derived from a ^{1}H-^{1}H ROESY spectrum of the Ac–RGD–NH_2 peptide reconstituted in DMSO-d_6 after lyophilization from an aqueous solution at pH 4.9. The ROESY spectrum was recorded at 310 K with a mixing time of 250 ms. The ROE intensities were converted into distances using the $\beta 1$-$\beta 2$ cross peak of Asp as reference. Thirty-six upper-limit cross-peak intensities, classified as strong (up to 2.8 Å), medium (up to 3.5 Å), and weak (up to 5 Å), were used as input restraints for the calculation. Appropriate corrections for center averaging were added to DYANA restraints for degenerate proton resonances.[23] No lower limits were used. Constraints for ψ, ψ, and χ^1 angles were calculated using the HABAS program of DYANA package. Six $^3J_{\alpha\beta 2}$ and $^3J_{\alpha}$ coupling constants were included with a tolerance of 2.5 Hz. All distance and angle constraints were assigned the default relative weight of 1. The default tolerance of 0.05 at target function units was applied. The calculations were performed using the standard minimization protocol and the REDAC (*RE*dundant *D*ihedral *A*ngle *C*onstraints) strategy implemented in DYANA.

RESULTS AND DISCUSSION

Conformational State of Ac–Arg–Gly–Asp–NH_2, Reconstituted in DMSO-d_6 from an Aqueous Solution at pH 2.0

The complete assignment of all proton resonances of Ac–Arg–Gly–Asp–NH_2 was based on the combined use of COSY, TOCSY, and ROESY experiments. The ^{1}H-NMR spectrum in DMSO-d_6 solution of the peptide reconstituted after lyophilization from an aqueous solution at pH 2 is shown in Figure 1 (bottom). The resonance at 12.3 ppm (not shown) confirms the protonated state of the Asp β-carboxylic group. The high absolute temperature coefficient values of all of the NH protons, including the C-terminal amide protons (−8 ppb/K), suggest that they are exposed to the solvent. The equal $^3J_{N\alpha}$ and $^3J_{N\alpha'}$ values (5.32 Hz) of Gly indicate that there is a free rotation about the N—C^{α} bond of this residue,[24] while the Asp $^3J_{\alpha\beta}$ and $^3J_{\alpha\beta'}$ coupling constant values (5.27 and 8.46 Hz) correspond to a high percentage (~80%, Table I) of the two energetically favored Cα–Cβ rotamers[25–28] (I and II, $\chi^1_{=}$ −60°, 180°), suggesting the absence of rotational restrictions about the C^{α}—C^{β} bond. On the other hand, the Arg–$N^{\varepsilon}H$ and Arg–$N^{\eta}_2H_4$ (this latter symbology indicates both N^{ε} atoms and all four protons linked to them) proton resonances, at 7.63 and 7.13 ppm, respectively, are attributed to their nonhydrogen-bonded states.[10,11,29] It must be noted that the Arg–$N^{\eta}_2H_4$ protons under free rotational conditions can be detected as two broad peaks due to chemical exchange in the guanidinium group.[10,11,30,31] In this conformational state two separate, broad peaks at 7.29

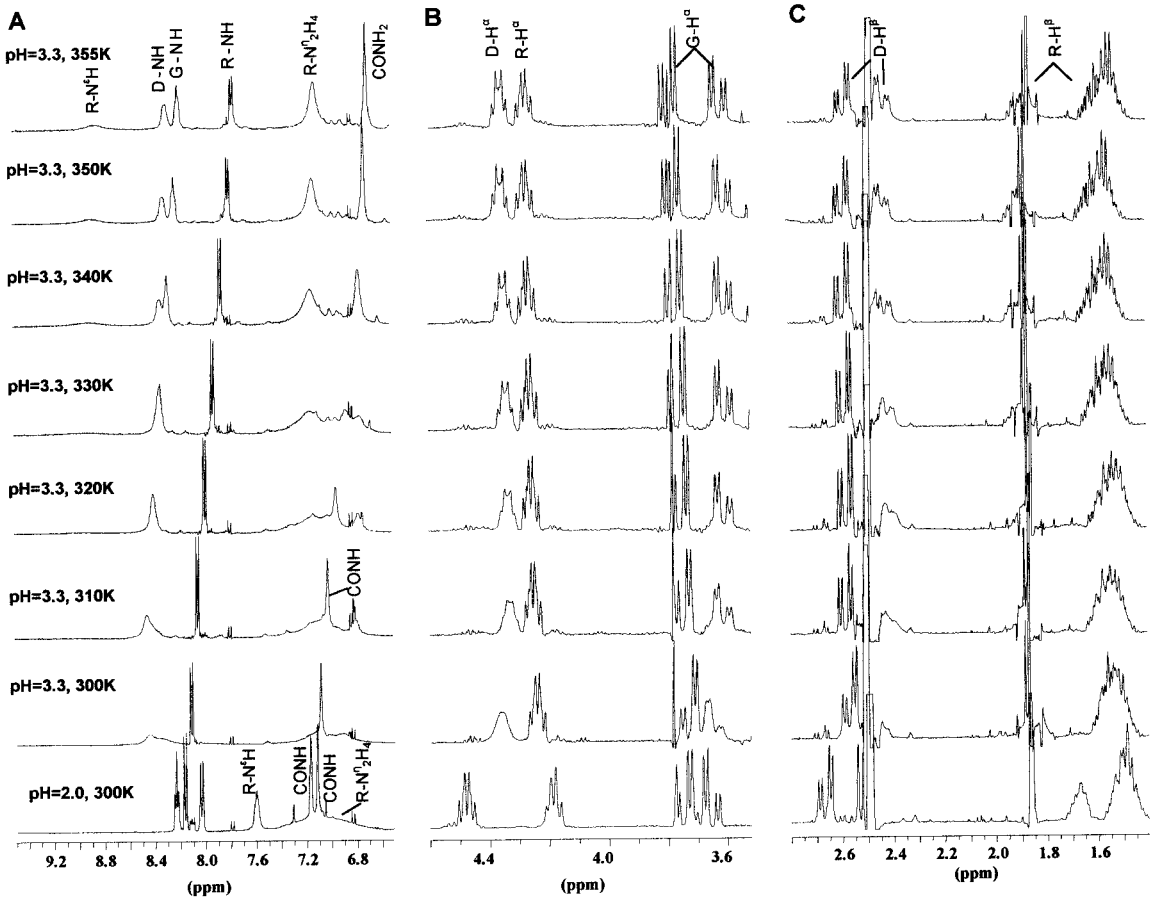

FIGURE 1 NH (A), $C^{\alpha}H$ (B), and $C^{\beta}H$ (C) regions of the 400 MHz ^{1}H-NMR spectra of Ac–RGD–NH_2 in DMSO-d_6 solution at various temperatures. Conformational reconstitution of the peptide was performed from an aqueous solution at pH 3.3. For comparison the spectrum of the peptide reconstituted from an aqueous solution at pH 2.0 is given (bottom). Arg–$N^{\eta}_2H_4$ notation indicates four protons.

and 6.91 ppm, respectively, were detected at 295 K (data not shown), which collapse to a broad peak at 300 K (Figure 1) at 7.13 ppm. Strong sharpening of this peak is observed as the temperature increases to 355 K (data not shown). The NMR data thus suggest that Ac–Arg–Gly–Asp–NH_2 is found in the extended conformational state when lyophilized from aqueous solution at pH 2 and redissolved in DMSO-d_6.

NMR spectra recorded back at 300 K after heating the sample to 355 K and keeping it at 300 K for varying time periods reveal the presence of a second set of resonances indicative of a slow aggregation process taking place under these conditions (data not shown). This conclusion is supported by the appearance in the ES-MS spectrum of a low intensity peak originating from a small amount of the dimeric form of the peptide. Interestingly, this peak was not detected under neutral or basic conditions (data not shown). Sanderson et al.[32] reported a similar observation for the (SS) Mba–Arg–Gly–Asp–Man peptide (Mba: 2-mercaptobenzoate; Man: 2-mercaptoanilide) in DMSO-d_6 solution. These authors, based on the fact that the Arg–$N^{\alpha}H$ was not detected in the second set of resonances, concluded that such a behavior could be the result of a slow hydrolytic process. This phenomenon can be excluded in our case by the full set of resonances for the Ac–Arg–Gly–Asp–NH_2 peptide present in the one-dimensional (1D) NMR spectrum and in the TOCSY and ROESY NMR spectra as well.

Conformational State of Ac–Arg–Gly–Asp–NH_2, in DMSO-d_6 Reconstituted from an Aqueous Solution at pH 3.3

The ionization state of the peptide remains the same as that at pH 2.0, as indicated by the presence of a broad peak at 12.25 ppm corresponding to the pro-

Table I Chemical Shift Differences of the Geminal Gly–$C^{\alpha}H_2$, Asp–$C^{\beta}H_2$, Arg–$C^{\beta}H_2$, Arg–$C^{\gamma}H_2$, and Arg–$C^{\delta}H_2$ Protons of Ac–Arg–Gly–Asp–NH_2 in DMSO-d_6 Solution at 300 K, Reconstituted from Aqueous Solutions at Various pH Values

	$\Delta\delta$ (ppm)							
						Rotamers[a] of the Asp C^{α}–C^{β} Bond (%)		
Conformational Reconstitution Solvent	Arg–$C^{\beta}H_2$	Arg–$C^{\gamma}H_2$	Arg–$C^{\delta}H_2$	Gly–$C^{\alpha}H_2$	Asp–$C^{\beta}H_2$	I	II	III
H_2O, pH = 2.0	0.15	~0.00	~0.00	0.08	0.16	26	54	20
H_2O, pH = 3.3	0.25	0.03	0.06	0.08	0.16[b]	25	31	44[b]
H_2O, pH = 4.0	0.36	0.04	0.11	0.20	0.35[c]	14	22	64[c]
H_2O, pH = 4.4	0.41	0.08	0.16	0.28	0.45	5	25	70[d]
H_2O, pH = 4.9	0.47	0.08	0.17	0.30	0.51	5	24	71

[a] Rotamer I ($\chi^1 = -60°$), II ($\chi^1 = 180°$), III ($\chi^1 = 60°$). The values of J_g and J_t used for estimation of the rotamer populations were 2.32 and 13.70 Hz, respectively.
[b] Measured at 340 K.
[c] Measured at 330 K.
[d] Measured at 310 K.

tonated form of the Asp β-COOH group. Nevertheless, the dramatic changes in the resonance frequencies and the line shapes over the entire spectrum are indicative of a new conformational state of the peptide. Thus, the Asp–NH proton broadens and is downfield shifted from 8.19 to 8.46 ppm, the Arg–$N^{\varepsilon}H$ becomes very broad and vanishes into the baseline at 300 K (Figure 1A), the Arg–$N^{\eta}_2H_4$ protons appear as a broad peak at 7.10 ppm, and the two carboxamide protons are seen as a sharp resonance at 7.10 ppm and a broad one at 6.92 ppm. The line shape of the resonances can provide information about the interacting parts of the molecule in the new conformational state. The observed broadening of many resonances is not due to a change in the rotational correlation time of the entire peptide since not all of the resonances are broadened to the same extent and the narrowing of each resonance occurs at different temperature values (Figure 1). Thus, the difference in the line width broadening of the Gly–NH, Asp–NH, Asp–$C^{\alpha}H$ resonances, the upfield shifted Gly–$C^{\alpha}H$, Asp–$C^{\beta}H$, and the C-terminal amide proton resonances, as well as the downfield shifted Arg–$C^{\beta}H$, indicate the occurrence of a slower exchange process, which affects mainly these groups, compared to the other parts of the molecule. It is also interesting to note that from the geminal Gly–$C^{\alpha}H_2$ and Asp–$C^{\beta}H_2$ protons, only the resonances of the upfield shifted protons appear broadened with that of the Asp–$C^{\beta}H$ proton almost vanishing into the baseline (Figure 1C). Since the Asp–$C^{\alpha}H$, Gly–$C^{\alpha}H$, Asp–$C^{\beta}H$, and the Arg–$C^{\beta}H$ protons cannot be involved in any other exchange process, we assume that the origin of their broadening resides in a conformational exchange process. It is also clear that the Gly–$C^{\alpha}H_2$ and Asp–$C^{\beta}H_2$ groups are not involved directly in the exchange process. Therefore, the differential broadening of their upfield shifted protons must originate from conformational interconversion of adjacent groups, which affects their local magnetic environment. Bogusky et al.[33] have reported a similar broadening for the Gly–$C^{\alpha}H_2$ protons brought about by freezing to $-80°C$ a methanolic solution of a cyclic (S,S) CRGDC peptide with a viscosity similar to that of DMSO at room temperature. In this case, molecular dynamics simulations have shown the presence of conformers differing by rotational inversions of the peptide-bond planes between the Arg–Gly and Gly–Asp residues.

The very fast interconverting rate between the conformers builds up gradually by raising the temperature from 300 to 350 K (Figure 1). The first groups of the molecule to achieve the very fast interconverting rate are located around Gly (at 310 K, Figure 1B). Most notable is the fact that at 330 K the upfield shifted Asp–$C^{\beta}H$ and especially the Arg–$N^{\varepsilon}H$ protons are still undergoing considerably slower exchange as revealed by their resonance broadening (Figures 1A, 1C, and 2). This finding probably indicates that there is a contact between the Arg–$N^{\varepsilon}H$ proton and the Asp β-COOH group responsible for this conformational exchange.

Besides the chemical shift changes observed between the conformational states reconstituted from pH 2.0 and 3.3, respectively, the temperature coefficient

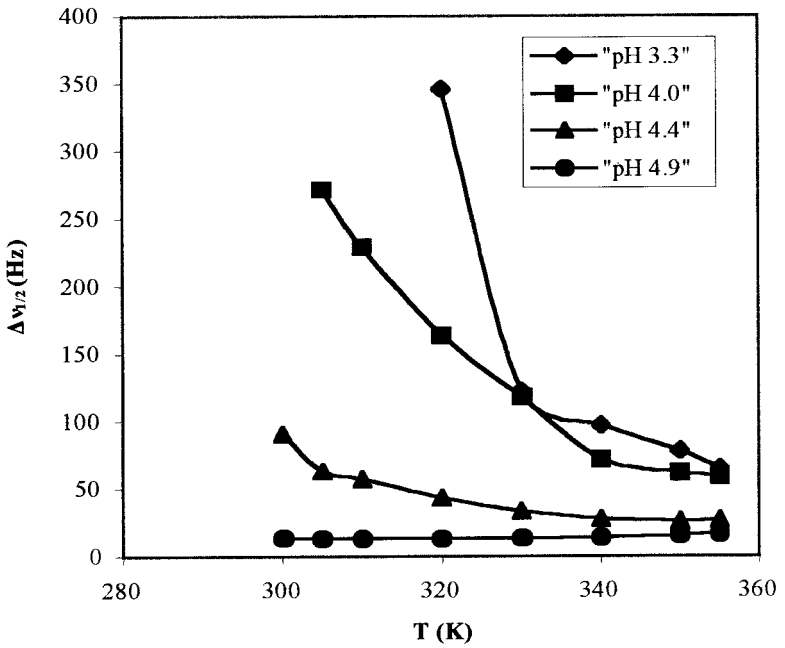

FIGURE 2 Plot of the Arg–N$^{\varepsilon}$H resonance line width ($\Delta\nu_{1/2}$) vs temperature of Ac–RGD–NH_2 in DMSO-d_6 solution reconstituted from aqueous solutions at different pH values.

values have been greatly modified in the latter case. Figure 3 shows the chemical shift variations with temperature of both C-terminal amide protons of Ac–RGD–NH_2 in DMSO reconstituted from solutions at several pH values. For comparison the same plot is also shown for the Ac–RGd–NH_2 peptide (which contains a D-Asp instead of L-Asp) under similar experimental conditions. The upfield shifted C-terminal amide proton is not accessible to the solvent, as judged by its low temperature coefficient value (−1.8 ppb/K) in the 310–330 K range. This is not true for the downfield shifted C-terminal amide proton (−7.5 ppb/K). It is evident from Figure 3 that temperature increase results in coalescence of the two resonances due to the increase of the rotational rate around the C-terminal primary amide bond, the double character of which is expected to be reduced in comparison to that of a secondary amide bond. The considerably higher temperature of coalescence (Figure 3) in Ac–RGD–NH_2 compared to Ac–RGd–NH_2 (more than 20°C), indicating a slower rotation around the C—N bond in the former case, can originate from conformational restrictions. Comparing the temperature coefficients in the temperature range 310–320 K and the temperatures of coalescence of the conformational states presented in Figure 3 we can safely conclude that the upfield shifted C-terminal amide proton is protected from the solvent for the states originating from aqueous solutions of the Ac–RGD–NH_2 peptide at pH 3.3 and 4.9. It is worth noting that similar low temperature coefficients for the upfield shifted amide proton were found previously for an Ac–Arg–Pro–Asp–NH_2 peptide.[12] A combination of NMR and molecular modeling data supported in that case the participation of this proton in hydrogen bonding with the Arg–CO group stabilizing a type I β-turn.

The broad peak of the Asp–NH of Ac–RGD–NH_2 in the temperature range of 300–330K and its overlapping with the resonance of the Gly–NH proton (Figure 4) does not allow an accurate determination of the temperature coefficient in this case.

As already mentioned, the Arg–N$^{\varepsilon}$H proton undergoes a conformational exchange at an intermediate rate up to 330 K. This is evidenced by the absence of a detectable peak. Raising the temperature from 330 to 355 K, a broad peak appears at ~8.92 ppm, which progressively sharpens (Figures 1A and 2). This behavior is indicative of a chemical exchange process, most probably between the hydrogen bonded and the open state. Taking into account that the Arg–N$^{\varepsilon}$H, the downfield shifted Arg–C$^{\beta}$H, and the upfield shifted Asp–C$^{\beta}$H proton resonances show a similar temperature dependent broadening, it is reasonable to assume that the Asp β-COOH would be the interacting group with the Arg–N$^{\varepsilon}$H proton. This hypothesis is further supported by the Asp $^3J_{\alpha\beta}$ and $^3J_{\alpha\beta'}$ coupling constant values (5.32 and 4.88 Hz, respectively) measured from the 1D high-resolution spectrum at 340 K. The reduced values indicate the presence of a high percentage (~44%, Table I) of the g^+ ($x^1 = 60°$)

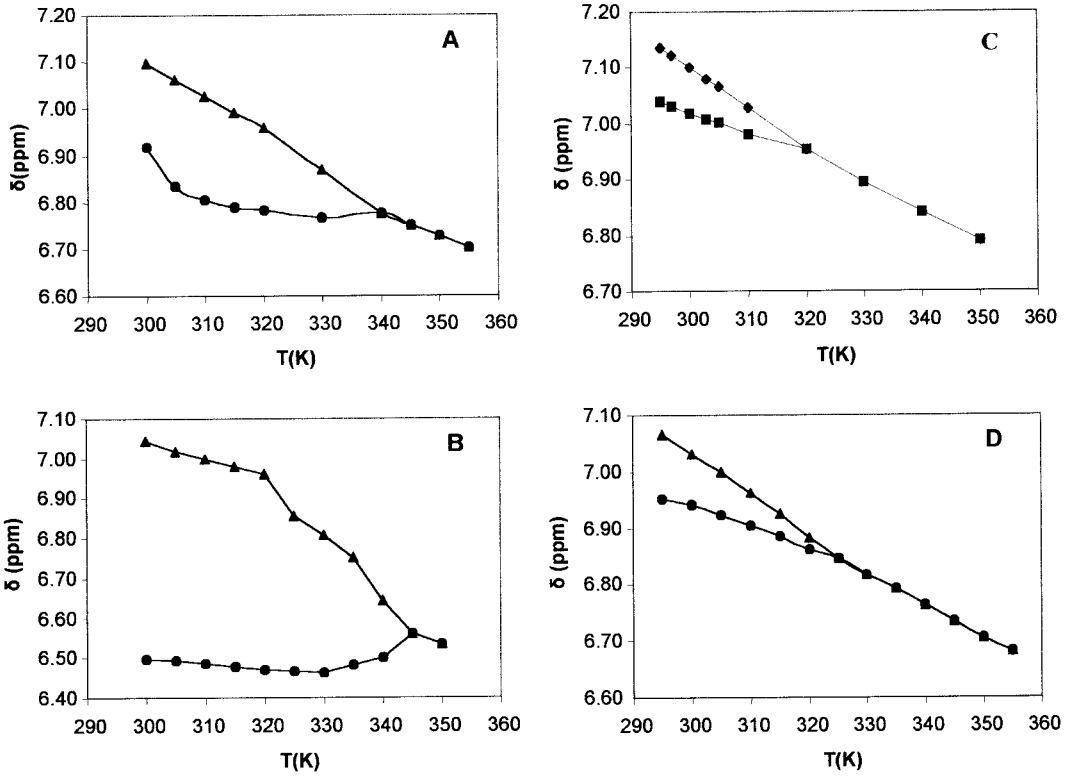

FIGURE 3 Plot of chemical shifts vs temperature of the C-terminal amide protons of Ac–RGD–NH_2 in DMSO-d_6 solution, reconstituted from aqueous solutions at pH 3.3 (A), pH 4.9 (B), and of Ac–RGd–NH_2 at pH 3.3 (C) and pH 4.9 (D).

rotational state about the C^{α}—C^{β} bond, which is the least energetically favored rotamer[25,28] under free rotational conditions. Comparing these data with those found for the Asp C^{α}—C^{β} rotational state at pH 2, we can conclude that conformational restrictions induce this unusual rotamer distribution. This is in agreement with the differential broadening of the two Asp–$C^{\beta}H$ resonances.

Although this intermediate conformational state appears stabilized by at least one hydrogen bond, the aliphatic parts of the Arg and Asp side chains still appear flexible. This is evident not only from the broadening of the Arg–$N^{\varepsilon}H$, the downfield shifted Arg–$C^{\beta}H$, and the upfield shifted of Asp–$C^{\beta}H$ protons, but also from the observed chemical shift differences for almost all the geminal Arg and Asp side-chain protons (Table I). These differences are small compared either to that observed in the case of the intermediate conformational state reconstituted from aqueous solution at pH 4.9 (see below, Table I) or to the reported data for the same side chains when they are involved in very strong interactions.[12]

Contrary to the behavior of the peptide at pH 2.0, the spectrum at pH 3.3 is completely recovered after heating at 355 K and annealing back to 300 K, indicating that there is no (or negligible) peptide aggregation in this case.

In short, at pH 3.3 the peptide seems to adopt a conformation distinctively different from that at pH 2.0, which appeared fully extended.

The observed changes in the NMR spectra of Ac–RGD–NH_2 for the conformational states reconstituted in DMSO from aqueous solutions at pH 4.0 and 4.4 further support the conformational analysis described above (Figure 4). More precisely, the guanidinium–β-carboxylate interaction seems enhanced, as judged by the following: (a) the further Arg–$N^{\varepsilon}H$ downfield shifting, (b) the broadening and upfield shifting of the Arg–$N_2^{\eta}H_4$ proton resonances, and (c) the gradual increase of the chemical shift difference between all the Arg and Asp side-chain geminal protons (Table I). The same proton resonances, as in the preceding conformational states (pH 3.3), appeared broadened, although their sharpening occurred at different temperature values. It must be noted that the Asp β-carboxylic proton resonance was detected as a very broad peak at pH 4.0, while it was no longer observed at pH 4.4.

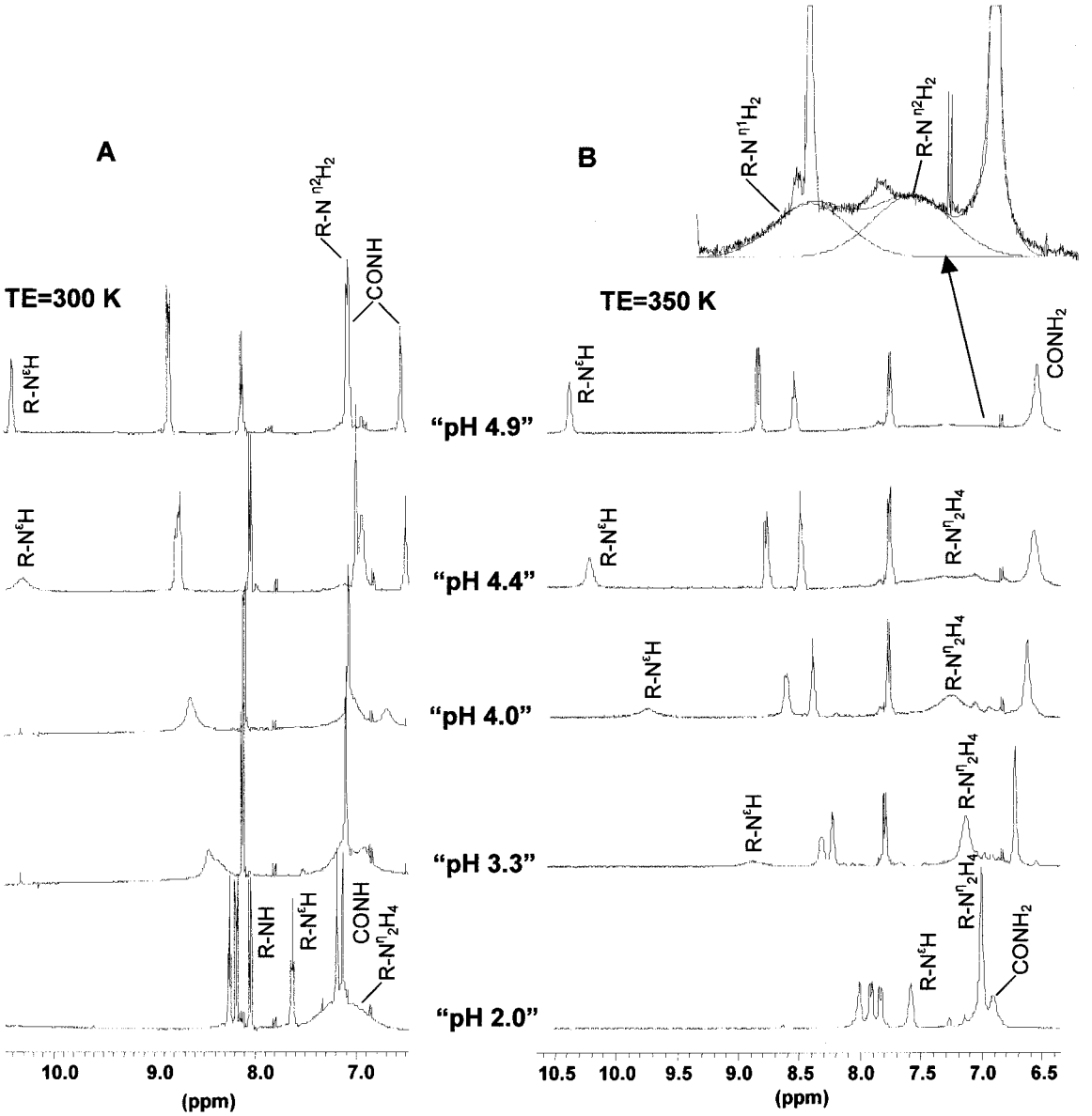

FIGURE 4 The 400 MHz ^{1}H-NMR spectra of the NH region of Ac–RGD–NH_2 in DMSO-d_6 solution, reconstituted from aqueous solutions at different pH values, at 300 K (A) and 350 K (B). The expanded spectrum of the Arg–$N^{\eta}_2H_4$ region in the *y* direction is also shown. Arg–$N^{\eta}_2H_4$ notation indicates four protons while Arg–$N^{\eta}H_2$ two protons.

Conformational State of Ac–Arg–Gly–Asp–NH_2 in DMSO-d_6 Reconstituted from Aqueous Solution at pH 4.9

The complete 1D spectrum of Ac–RGD–NH_2 in DMSO-d_6 after reconstitution from an aqueous solution at pH 4.9 is shown in Figure 5B. Although the changes in the spectrum tend to confirm the previous conformational analysis, almost all of the resonances are very sharp in this case. More specifically, the strong downfield shifting of the Arg–$N^{\varepsilon}H$ proton and the substantial chemical shift differences between the Asp–$C^{\beta}H_2$, Arg–$C^{\beta}H_2$, and Arg–$C^{\delta}H_2$ geminal protons (Table I) point to a further stabilization of the conformation that involves the interaction between the Arg and Asp side chains. Taking into account that the Asp β-COO^- group is now in the deprotonated form, it is reasonable to expect that ionic forces contribute to this stabilization. On the other hand, the overall appearance of the spectrum, with only one set of resonances clearly present, and the sharpness of all

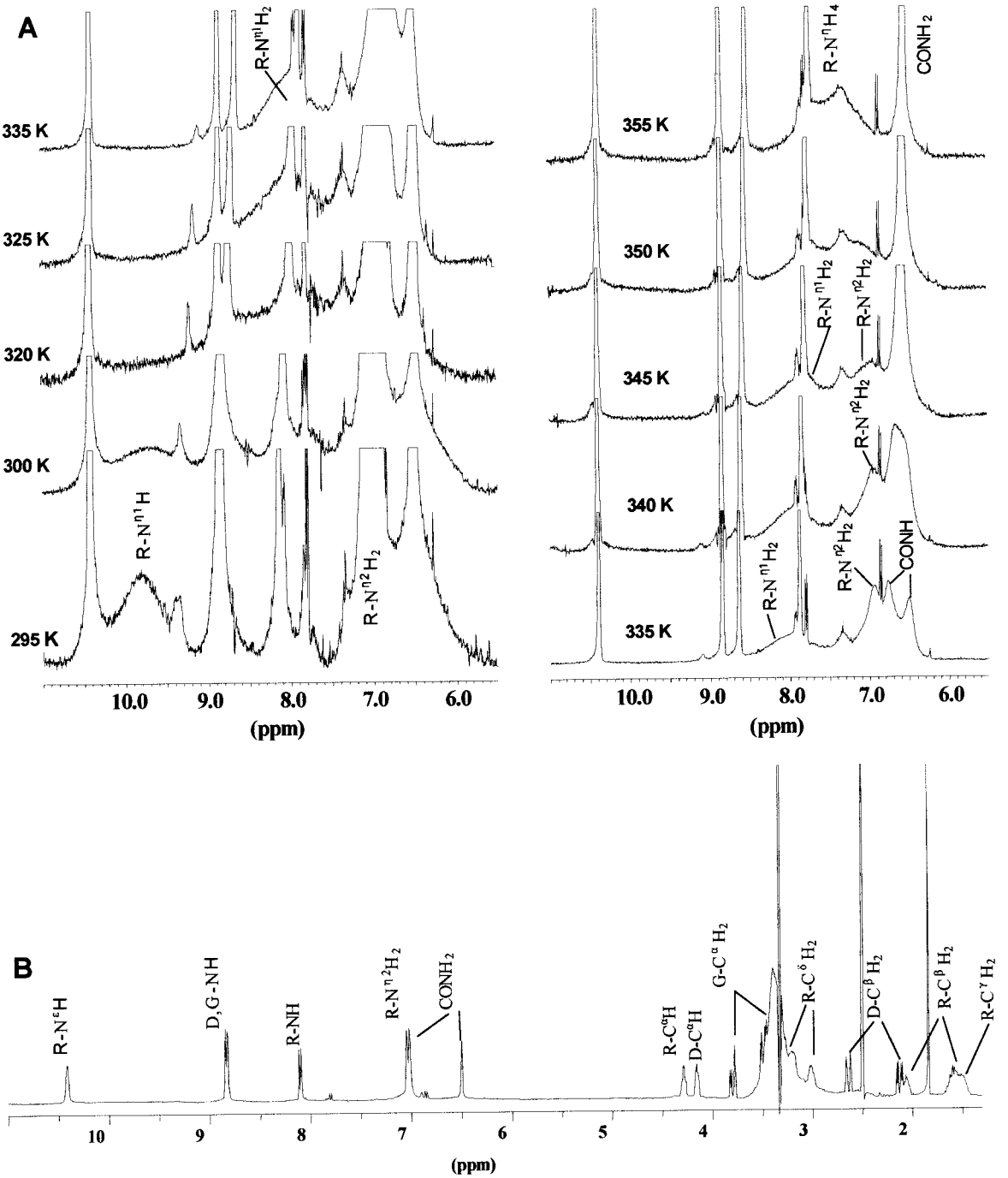

FIGURE 5 The 400 MHz ^{1}H-NMR spectra of the NH region of Ac–RGD–NH_2 in DMSO-d_6 solution, reconstituted from an aqueous solution at pH 4.9, at different temperatures (A). The complete spectrum of Ac–RGD–NH_2 at pH 4.9 and 300 K is shown at the bottom (B). Notation as in Figure 4.

peaks, hint to either a very fast exchange process between folded and unfolded states or to a very slow conformational exchange with the equilibrium quantitatively shifted toward the folded state. From these observations the following questions may be addressed: Is there any conformational exchange process taking place under these experimental conditions? If so, what is the rate of this process?

To answer these questions, we relied on the monitoring and the detailed analysis of the behavior of

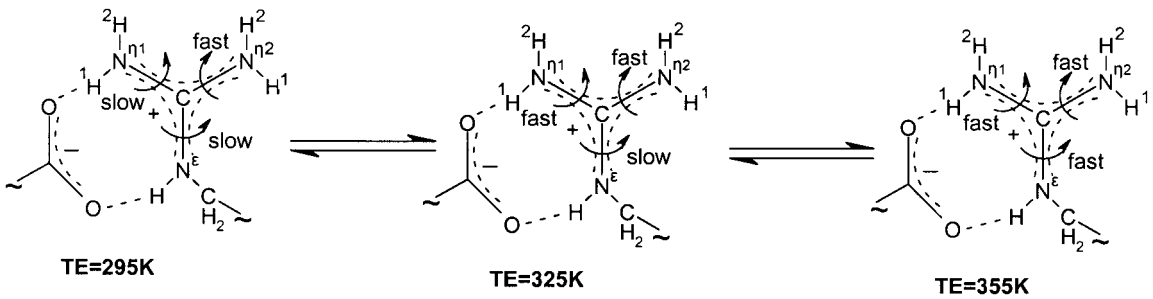

FIGURE 6 Proposed rotational pattern of the guanidinium N^{ε}–C^{ζ}, C^{ζ}–$N^{\eta 1}$ and C^{ζ}–$N^{\eta 2}$ bonds of Ac–RGD–NH_2 in the intramolecular hydrogen-bonded interaction with Asp β-COO^- according to the experimental 400 MHz ^{1}H-NMR data.

several resonances at different pH and temperature values. In this respect the resonances originating from the Arg–$N^{\eta}H_4$ protons provided the most valuable information. Comparing the 1D spectra of Ac–RGD–NH_2 recorded in DMSO-d_6 after reconstitution from aqueous solutions at pH 2.0, 3.3, 4.0, 4.4, and 4.9 (Figure 4), it is evident that the Arg–$N^{\eta}H_4$ protons contribute progressively, but differently, to the structure stabilization.

Two protons of Arg–N^{η}, when reconstitution takes place at pH 4.9, appear as a sharp resonance at 7.01 ppm at 300 K, whereas the other two protons are almost not detectable (Figure 5A). However, the spectrum recorded at 295 K, when expanded in the *y* direction, reveals the presence of a broad peak at 9.78 ppm (Figure 5A). By increasing the temperature, this peak broadens and cannot be detected in the temperature range of 305–325 K. Up to this temperature the resonance at 7.01 ppm slightly broadens and shifts upfield (from 7.01 to 6.94 ppm). At 325 K a new broad peak appears at 8.05 ppm, which sharpens when the temperature is increased to 335 K. Obviously, this new peak is the result of coalescence between two peaks. The chemical shift of the second broad, unresolvable at 295–300 K, peak, calculated from the chemical shifts of the peaks at 9.78 and 8.05 ppm, was found centered at 6.28 ppm. The 1D 500 MHz spectrum at 295 K confirms the presence of the second upfield shifted broad peak at around 6.45 ppm, in good agreement with our calculated value. Upon further heating to 355 K, the new peak at 8.05 ppm and the sharp one at 6.94 ppm become progressively equivalent, broaden, and coalesce at 7.40 ppm (Figure 5A).

If the downfield shifting of the Arg–$N^{\varepsilon}H$ proton, due to its participation in hydrogen bonding, is also taken into account, the chemical shift dispersion of the guanidinium group can be explained according to the scheme depicted in Figure 6. Thus, the very fast rotation around the C^{ζ}–$N^{\eta 2}$ bond could explain the sharp resonance observed for the two Arg–$N^{\eta 2}H$ protons at 7.01 ppm. The very slow rotation around the bond C^{ζ}–$N^{\eta 1}$ resulting from hydrogen bonding could give rise to two separate peaks at 9.78 and 6.45 ppm. The hydrogen bonding of both the Arg–$N^{\eta 1}H^1$ and Arg–$N^{\varepsilon}H$ protons are possibly responsible for the slow rotation around the N^{ε}–C^{ζ} bond. As the temperature increases, the rotation around the C^{ζ}–$N^{\eta 1}$ becomes fast due to hydrogen-bond breaking, resulting in the appearance of a broad peak at 8.05 ppm for the two Arg–$N^{\eta 1}H$ protons at 325 K. Increase of the rate of rotation around the N^{η}–C^{ζ} bond leads to the equivalence of the two Arg–$N^{\eta}H_2$ groups with a new coalescence of the resonances at 7.40 ppm at 355 K.

A three-step resonance coalescence between Arg–$N^{\eta 1}H^1$/Arg–$N^{\eta 1}H^2$, Arg–$N^{\eta 2}H^1$/Arg–$N^{\eta 2}H^2$, and Arg–$N^{\eta 1}H_2$/Arg–$N^{\eta 2}H_2$ at temperature values of 238, 246, and 303 K, respectively, has also been reported in the past for the Arg–$N^{\eta}_2H_4$ protons of Ac–Arg(HCl)O^{i}Pr (O_iPr: isoproxy) in a 5:95 DMSO/CD_2Cl_2 (v/v) solution at 400 MHz.[30]

In the case of intermolecular interaction of Arg–guanidinium with ligand carboxylate groups, four NMR signals were observed for the four $N^{\eta}H$ protons.[34,35] The two lowest ^{1}H signals (9.33 and 10 ppm) assigned to $NH^{\eta 12}$ and $NH^{\eta 22}$ were attributed to their hydrogen bonding with the ligand carboxylate oxygens. At 313 K the high field pair of signals coalesced into a single broad signal, but the coalescence temperature for all four guanidinium protons was not resolved. This pattern was attributed to a fast rotation about the N^{ε}–C^{ζ} bond, but to a slow rotation about the C^{ζ}–N^{η} bond, on the NMR chemical shift time scale.

In our study the coalescence temperatures at 400 MHz for Arg–$N^{\eta 1}H^1$/Arg–$N^{\eta 1}H^2$, and Arg–$N^{\eta 1}H_2$/Arg–$N^{\eta 2}H_2$ are considerably higher compared either to the free Arg or the one complexed to a carboxylate ligand, suggesting slower rotation rates around the C^{ζ}–$N^{\eta 1}$ and N^{ε}–C^{ζ} bonds. The reversed chemical shift and rotation pattern about the N^{ε}–C^{ζ} and C^{ζ}–N^{η}

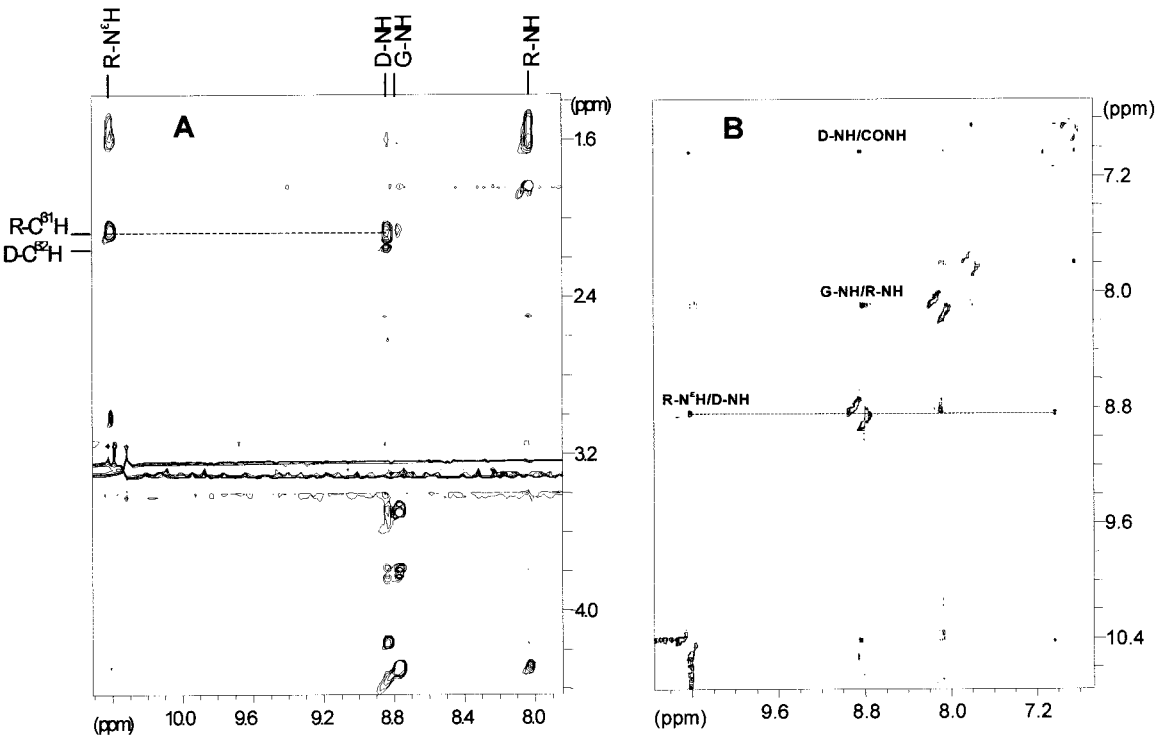

FIGURE 7 The NH/C$^{\alpha}$H (A) and NH/NH (B) regions of the 400 MHz ROESY spectrum of Ac–RGD–NH_2 in DMSO-d_6, reconstituted from an aqueous solution at pH 4.9, at 310 K and t_m = 250 ms.

bonds found for Ac–RGD–NH_2 is consistent with the Arg–N$^{\varepsilon}$H and Arg–N$^{\eta1}$H^{1} (Figure 6) hydrogen-bonded interaction. Interestingly, it has been proposed in the past[36] that Arg–N$^{\varepsilon}$H and Arg–N$^{\eta1}$ protons participate in intramolecular interactions, while Arg–N$^{\eta1}$ and Arg–N$^{\eta2}$ protons are more often involved in intermolecular interactions.

The occurrence of a guanidinium–carboxylate interaction, which is responsible for the restricted rotation about the N$^{\varepsilon}$–C$^{\zeta}$ and C$^{\zeta}$–N$^{\eta1}$ bonds, is further supported by the behavior of the Arg and Asp side chains, as well as by the observed ROE effects. Thus, the Arg and Asp side-chain geminal protons exhibit unusually strong chemical shift differences (Table I), probably as a result of their restricted mobility. In addition, the Asp $^{3}J_{\alpha\beta1}$ and $^{3}J_{\alpha\beta2}$ coupling constant values (2.85 and 5.29 Hz, respectively) indicate a very high percentage (~71%) of the less energetically favored rotamer g^{+} (x^{1} = 60°) (Table I). Under these rotational conditions one of the β-COO^{-} oxygens must be oriented in close proximity to the Asp–NH proton.[25] This fact can explain the low absolute temperature coefficient observed for the Asp–NH (~0 ppb/K). At the same time, the hydrogen bonding of the Arg–N$^{\varepsilon}$H with the Asp β-COO^{-} group would bring this proton in the proximity of the Asp–NH. This result is clearly confirmed by the observed ROE effects between Arg–N$^{\varepsilon}$H/Asp–NH and Arg–C$^{\beta2}$H/Asp–NH protons (Figure 7). These ROE effects were accurately resolved by recording the ROESY spectrum at 310 K in order to overcome the overlapping of Asp–NH and Gly–NH resonances. Table II indicates the number of the observed ROE effects for the Ac–RGD–NH_2 in DMSO-d_6 solution when the reconstitution was performed in aqueous solution at pH 4.9. The numerous ROEs detected for this small molecule strongly suggest that its conformation is very compact. In agreement with this finding are also the small absolute temperature coefficient values measured for the Asp–NH (~0 ppb/K), the upfield shifted —$CONH_2$ (−1.3 ppb/K in the temperature range 300–325 K), and the behavior of the Arg–N$^{\varepsilon}$H proton resonance. It is interesting to note that, in contrast to the conformational states reconstituted from aqueous solution at pH 2.0 and 3.3, in this case the line width of the Arg–N$^{\varepsilon}$H resonance remains unchanged on heating to 355 K (Figure 2). This finding suggests that the hydrogen-bonded network and the ionic interaction, which stabilizes the structure, are very strong, and there is no conformational exchange involving breaking of the hydrogen bond between Arg–N$^{\varepsilon}$H and Asp β-COO^{-} even at temperatures as high as 355 K.

Table II Classification of Restraints and Structure Statistics

Restraint Classification	
Total number of NOEs	36
Number of backbone–backbone NOEs	10
Number of backbone–side-chain NOEs	23
Number of side-chain–side-chain NOEs	3
Number of intraresidue NOEs	13
Number of interresidue NOEs	23
Number of strong NOEs (<2.8 Å)	4
Number of medium NOEs (<3.5 Å)	11
Number of weak NOEs (<5 Å)	21
Total number of *J*	6
Number of $^3J_{N\alpha}$	4
Number of $^3J_{\alpha\beta}$	2
Number of hydrogen bonds	2
Calculation Results	
Number of structures calculated	100
Number of final structures	10
Min/max target function of final structures	$1.79/5.56 \times 10^{-2}$
Number of distance restraint violations > 0.3 Å	0
Number of distance restraint violations > 0.2 Å	1 (in 3/10 structures)
Number of torsion angle violations	0
Mean global heavy atom RMSD	0.68 ± 0.26 Å
Mean global backbone RMSD	0.37 ± 0.13 Å

Based on the data just described and their detailed analysis, we conclude that the Ac–RGD–NH_2 peptide when reconstituted in DMSO from pH 4.9 quantitatively adopts a very stable and folded conformation, which undergoes an unusually slow exchange with the extended conformation.

Rates of Rotation About the N^{ε}–C^{ζ}, C^{ζ}–$N^{\eta 1}$, and C^{ζ}–$N^{\eta 2}$ Bonds

Depending on the environment and the nature of the interactions involving the guanidinium protons, various patterns can be observed for the rotation rates around the N^{ε}–C^{ζ} bond. Under free rotational conditions the Arg residue shows a single broad, coalesced resonance for $N^{\eta 1}H_2$ and $N^{\eta 2}H_2$ protons in the 400 MHz ^{1}H-NMR spectrum in DMSO-d_6 solution at 300 K. (See Figure 1.) The coalesced signal arises from exchange between the N^{η} H protons caused by rotations about the N^{ε}–C^{ζ} and C^{ζ}–N^{η} bonds. For Ac–Arg–O^{i}Pr in 5:95 DMSO/CD_2Cl_2 (v/v) solution at 298 K, rates of 130, 7800, and 17500 s^{-1} for N^{η}–C^{ζ}, C^{ζ}–$N^{\eta 1}$, and C^{ζ}–$N^{\eta 2}$ bond rotations, respectively, have been reported.[30] The rates of N^{ε}–C^{ζ} and C^{ζ}–N^{η} bond rotations are dramatically reduced for an Arg complexed to a ligand carboxylate group in which both $N^{\eta 1}H_2$ and $NH^{\eta 2}H_2$ groups are involved in stable hydrogen-bonding interactions.[35] This is the case of *L. casei* dihydrofolate reductase (DHFR) complexed either with methotrexate (MTX) or with MTX and β-nicotinamide adenine dinucleotide phosphate (NADPH). The rates about the $N^{\varepsilon}C^{\zeta}$ and $C^{\zeta}N^{\eta}$ bonds were found to be 565 and <117 s^{-1} for the DHFR · MTX complex, and 930 and <71 s^{-1} for the DHFR · MTX · NADPH complex, respectively, at 313 K.

Based on the scheme depicted in Figure 6, an altered pattern for the rotation rates about the N^{ε}–C^{ζ} and C^{ζ}–N^{η} bonds is expected for our peptide in comparison to that of the DHFR complexes. The rates of rotation about the N^{ε}–C^{ζ}, C^{ζ}–$N^{\eta 1}$, and C^{ζ}–$N^{\eta 2}$ bonds estimated from temperature- dependent line shape analysis are 10, 642, and 5350 s^{-1}, respectively, at 295 K. The rates for the N^{ε}–C^{ζ} and C^{ζ}–$N^{\eta 1}$ bond rotations are 13-fold lower than the corresponding rates reported for Ac–Arg–O^{i}Pr[30] in a 5:95 DMSO/CD_2Cl_2 (v/v) solution at 298 K. On the contrary, the rate for the C^{ζ}–$N^{\eta 2}$bond rotation, the group that does not participate in a hydrogen-bonded interaction, is only 3-fold lower.

The most surprising finding in this study is that, even at 355 K, the hydrogen-bonded interactions between the guanidinium and carboxylate groups are still strong enough, resulting in a rate of rotation about the N^{ε}–C^{ζ} bond of 561 s^{-1}. Especially, the hydrogen-bonded interaction involving the Arg–N^{ε}H proton is very stable, as evidenced by the slight broadening (~20%) of the resonance on heating to 355 K. The Eyring diagram yields the activation parameters, for rotation about the N^{ε}–C^{ζ} bond, $\Delta H^* = 56.4$ kJ mol^{-1}, $\Delta S^* = -35.8$ J · mol^{-1}, and $\Delta G^*(303) = 67.3$ kJ mol^{-1}. The free energy of activation for the N^{ε}–C^{ζ} bond rotation is significantly higher in our case than that estimated for the same bond (61 kJ mol^{-1}) in Ac–Arg–O^{i}Pr in a 5:95 DMSO/CD_2Cl_2 (v/v) solution[30] or for Arg (54 kJ mol^{-1}) in a 50% aqueous DMSO solution.[31] The increased value of ΔG^* is probably the result of the guanidinium hydrogen-bonded interactions.

Structure Calculation

The structure of the Ac–RGD–NH_2 peptide in DMSO-d_6 reconstituted from pH 4.9 was calculated on the basis of 36 upper distance constraints and 6

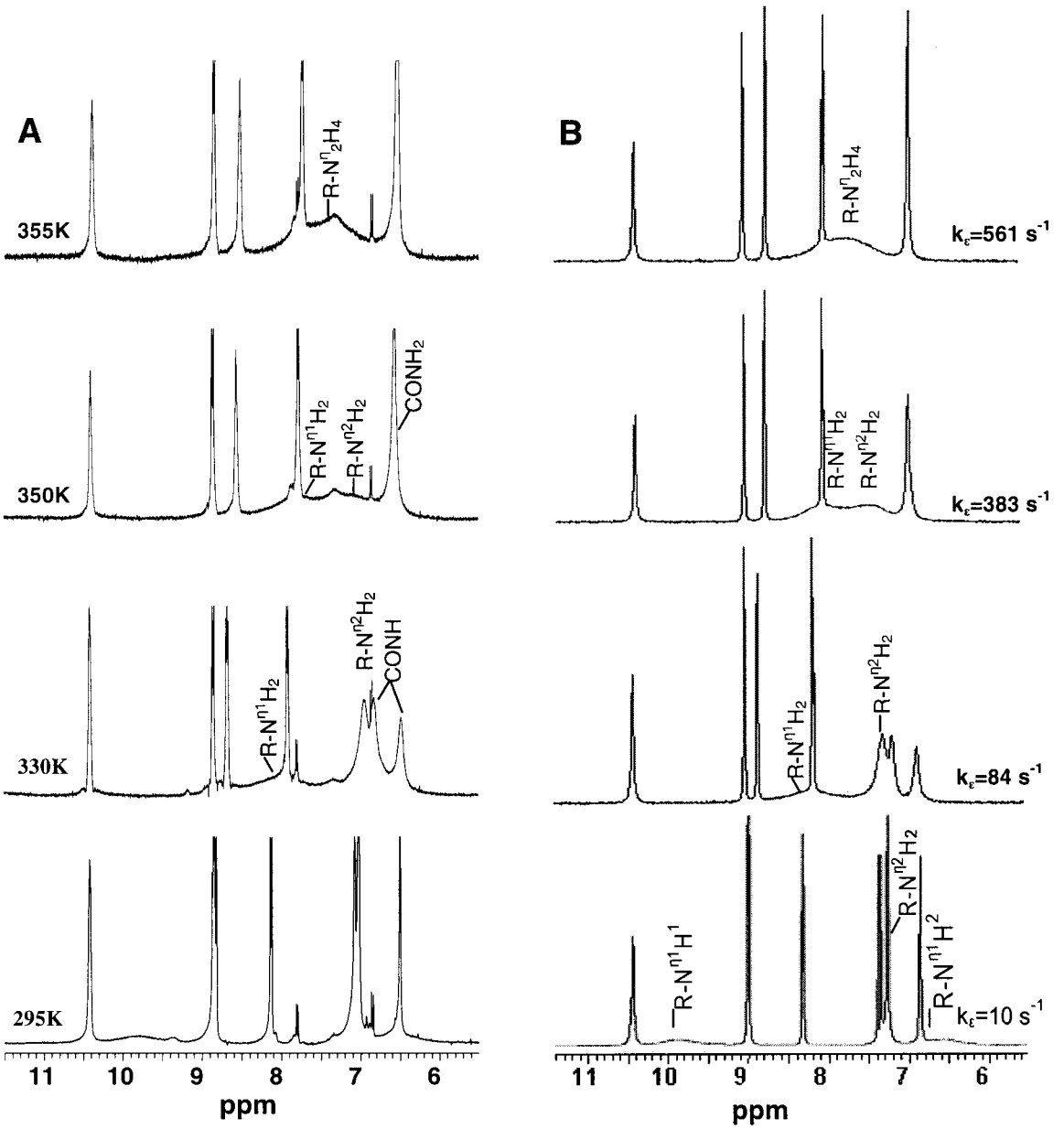

FIGURE 8 Experimental 400 MHz NMR (A) and calculated spectra of the Ac–RGD–NH_2 in DMSO-d_6 solution reconstituted from an aqueous solution at pH 4.9 (B). For each pair of experimental and calculated spectra, the experimental temperature is indicated. The rotation rate about the N^{ε}–C^{ζ} bond (k_ε) is also shown. Notation as in Figure 4.

torsion angle constraints using the REDAC strategy of the DYANA software.[22] Of the 100 structures generated by DYANA, the best 10 were selected on the basis of their target functions and the low number of restraint violations. After a first run of REDAC, two side-chain–side- chain hydrogen bonds were imposed from those present in at least 3 out of the 10 best resulting structures between Arg–$N^{\varepsilon}H$ and Arg–$N^{\eta 1}H_2$ (donors) and Asp β-COO^- (acceptor). When these hydrogen bonds were added as upper distance constraints to a second run of DYANA, the number of violated distance constraints was reduced from 3 to 1, and a new hydrogen bond present in over half of the 10 best structures was identified between Arg–$N^{\eta 1}H_2$ and Asp–CO. No dihedral angle violation was observed. The final 10 structures were characterized by very low target functions, the absence of any violations $>$0.3 Å, and relatively low root mean square

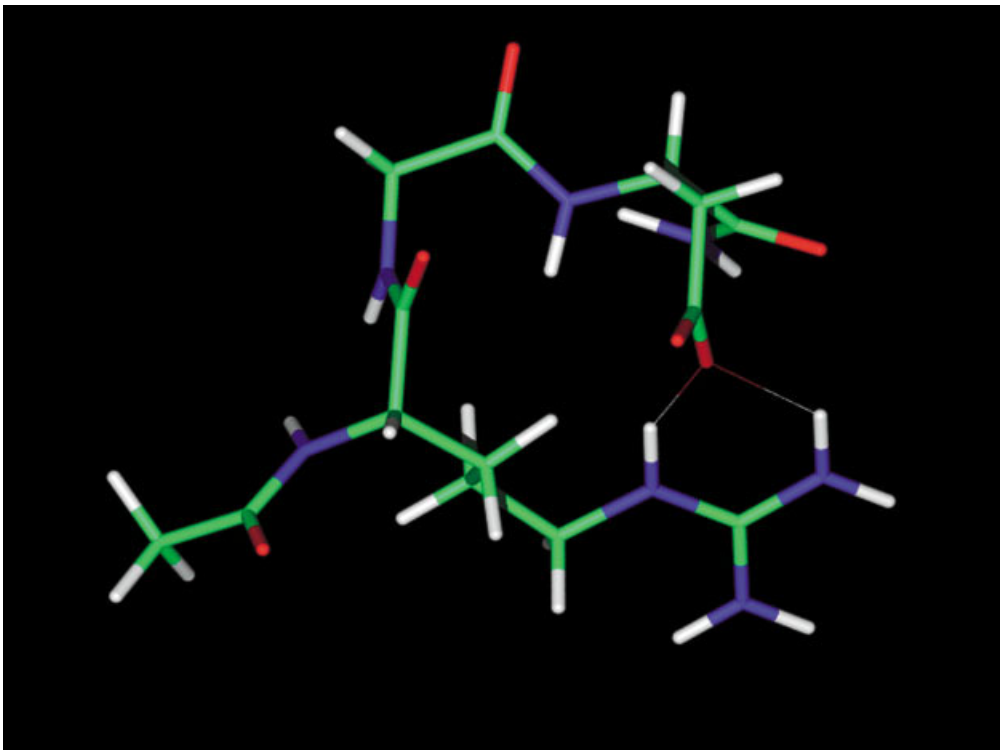

FIGURE 9 Best structure (the one with the lowest value of target function) calculated with use of the REDAC strategy of DYANA. Thin lines represent hydrogen bonds.

displacement (RMSD) values. A classification of the experimental restraints and a statistical analysis of the best 10 of the calculated structures are given in Table II.

The elements of intramolecular structuring indicated by the conformational analysis presented in detail above and summarized in the model depicted in Figure 6 are confirmed by the calculated structure (Figure 9). The existence of a compact "pseudocyclic" structure stabilized by hydrogen bonding in a head-to-tail fashion, also supported by previous work with peptides having an Arg residue in the third position from the C-terminus,[9–12] is consistent with the pattern of hydrogen bonds resulting from the calculations. More specifically: (a) there seems to be a bifurcated hydrogen bond between the Asp β-COO^- and the Arg–N^{ε} and one of the Arg–$N^{\eta 1}$ protons; (b) the conformation might be even more stabilized through an additional interaction of the guanidinium group with the terminal carbonyl group of Asp; (c) the *trans* proton of the C-terminal NH_2 group is pointing to the interior of the pseudocyclic structure in more than half of the best 10 structures, being thus shielded from the solvent, as also indicated by its temperature coefficient values; (d) the compactness of the peptide conformation is confirmed by the short distances in all calculated structures between the Asp–NH proton and the Arg–N^{ε} ($\leq$3.2 Å) and Arg–$C^{\beta 2}H$ ($<$2.7 Å) protons, due to the restricted mobility of these side chains.

CONCLUSIONS

In this study, focused on the Ac–RGD–NH_2 peptide as a model system, we provided experimental evidence for some important general aspects related to the conformational states of short linear peptides in solution. The novel information deduced from this work can be summarized as follows:

The discrete conformational states of the peptides in DMSO-d_6 can undergo very slow exchange. Thus, the species normally observed by NMR might represent only local conformational changes, which are fast in the NMR time scale, rather than an overall average structure.

The approach based on the rational selection of the conditions employed before the conformational reconstitution of a peptide in DMSO allows a more accurate characterization of its folded structure and of the folding process, since the driving interactions and forces become in this manner more discernible and can be quite easily evaluated. Moreover, the hypothesis that short linear peptides in solution are found in fast conformational exchange in the NMR time scale

is not always valid, and has to be explored and verified in each separate case.

Intramolecular hydrogen-bonding interactions can persist and stabilize the conformation of short linear peptides even at very high temperatures.

The folded structure in DMSO-d_6, of Ac–RGD–NH_2, is characterized by an ionic bridge between Arg guanidinium and Asp β-carboxylate groups. Two hydrogen bonds involving the Arg–$N^{\varepsilon}H$ and Arg–$N^{\eta}H$ protons stabilize the interaction between the oppositely charged groups.

This work was supported by a grant from the Greek Secretariat of Research and Technology. The authors thank V. I. Polshakov for providing the program Muses.

REFERENCES

1. Eggleston, D. S.; Feldman, S. H. Int J Pept Protein Res 1990, 36, 161–166.
2. Kang, Y. K.; Jhon, J. S. J Pept Res 2000, 56, 360–372.
3. Bogdanowich,-Knipp, S. J.; Jois, S. D.; Siahaan, T. J. J Pept Res 1999, 53, 523–529.
4. Aubry, A.; Birlirakis, N.; Sakarellos-Daitsiotis, M.; Sakarellos, C.; Marraud, M. Biopolymers 1989, 28, 27–40.
5. Aubry, A.; Birlirakis, N.; Sakarellos-Daitsiotis, M.; Sakarellos, C.; Marraud, M. J Chem Soc, Chem Commun 1988, 963–964.
6. Brockwell, D. J.; Smith, D. A.; Radford, S. E. Curr Opin Struct Biol 2000, 10, 16–25.
7. Volk, M. Eur J Org Chem 2001, 2605–2621.
8. Eaton, W. A.; Munoz, V.; Thompson, P. A.; Henry, E. R.; Hofrichter, J. Acc Chem Res 1998, 31, 745–753.
9. Sakarellos-Daitsiotis, M.; Panou-Pomonis, E.; Sakarellos, C.; Cung, M. T.; Marraud, M.; Tzinia, A. K.; Soteriadou, K.; Tsikaris, V. Lett Pept Sci 1996, 3, 200–208.
10. Tsikaris, V.; Sakarellos-Daitsiotis, M.; Panou-Pomonis, E.; Detsikas, E.; Sakarellos, C.; Cung, M. T.; Marraud, M. Pept Res 1992, 5, 110–114.
11. Tsikaris, V.; Cung, M. T.; Panou-Pomonis, E.; Sakarellos, C.; Sakarellos-Daitsiotis, M. J Chem Soc, Perkin Trans 2 1993, 1345–1349.
12. Tsikaris, V.; Sakarellos-Daitsiotis, M.; Tzovaras, D.; Sakarellos, C.; Orlewski, P.; Cung, M. T.; Marraud, M. Biopolymers 1996, 38, 673–682.
13. Tsikaris, V.; Moussis, V.; Sakarellos-Daitsiotis, M.; Sakarellos C. Tetrahedron Lett 2000, 41, 8651–8654.
14. Boden, N.; Cheng, Y.; Knowles, P. F. Biophys Chem 1997, 65, 205–210.
15. Pierschbachter, M. D.; Ruoslahti, E. Nature 1984, 308, 30–33.
16. Suzuki, S.; Oldberg, A.; Hayman, E. G.; Pierschbachter, M. D.; Ruoslahti, E. EMBO J 1985, 4, 2519–2524.
17. Watt, K. W. K.; Cottrall, B. A.; Strong, D. D.; Doolitle, R. F. Biochemistry 1979, 18, 5410–5416.
18. Stavrakoudis, A.; Bizos, G.; Elefteriadis, D.; Kouki, A.; Panou-Pomonis, E., Sakarellos-Daitsiotis, M.; Sakarellos, C.; Tsoukatos, D.; Tsikaris, V. Biopolymers 2001, 56, 20–26.
19. Stewart, J. M.; Young, J. D. Solid Phase Peptide Synthesis; Pierce Chemical Company: Rockford, IL, 1984.
20. Sandström, J. Dynamic NMR Spectroscopy; Academic Press: London, 1982.
21. Polshakov, V. I.; Birdsal, B.; Feeney, J. Biochemistry 1999, 38, 15962–15969.
22. Guntert, P.; Mumenthaler, C.; Wüthrich, K. J Mol Biol 273 1997, 283–298.
23. Wüthrich, K.; Billeter, M.; Braun, W. J Mol Biol 1983, 169, 949–961.
24. Tsikaris, V.; Detsikas, E.; Sakarellos-Daitsiotis, M.; Sakarellos, C.; Vatzaki, E.; Tzartos, S. J.; Marraud, M.; Cung, M. T. Biopolymers 1993, 33, 1123–1134.
25. Benedetti, E.; Morelli, G.; Nemethy, G.; Scheraga, H. A. Int J Pept Protein Res 1983, 22, 1–15.
26. De Leeuw, F. A. A. M.; Altona, C. Int J Pept Protein Res 1982, 20, 120–125.
27. Cung, M. T.; Marraud, M. Biopolymers 1982, 21, 953–967.
28. McGregor, M. J.; Islam, S. A.; Sternberg, M. J. J Mol Biol 1987, 198, 295–310.
29. Mayer, R.; Lancelot, G. J Am Chem Soc 1981, 103, 4738–4742.
30. Smith, R. J.; Williams, D. H.; James, K. J Chem Soc, Chem Commun 1989, 682–683.
31. Kanamori, K.; Roberts, J. D. J Am Chem Soc 1983,105, 4698–4701.
32. Sanderson, P. N.; Glen, R. C.; Payne, A. W. R.; Hudson, B. D.; Heide, C.; Tranter, G. E.; Doyle, P. M.; Harris, C. J. Int J Pept Protein Res 1994, 43, 588–596.
33. Bogusky, M. J.; Naylor, A. M.; Pitzenberger, S. M.; Nutt, R. F.; Brady, S. F., Colton, C. D.; Sisko, J. T.; Anderson, P. S.; Veber, D. F. Int J Pept Protein Res 1992, 39, 63–76.
34. Gargaro, A. R.; Frenkiel, T. A.; Nieto, P. M.; Birdsall, B.; Polshakov, V. I.; Morgan, W. D.; Feeney, J. Eur J Biochem 1996, 238, 435–439.
35. Nieto, P. M.; Birdsall, B.; Morgan, W. D.; Frenkiel, T. A.; Gargaro, A. R.; Feeney, J. FEBS Lett 1997, 405, 16–20.
36. Mitchell, J. B. O.; Thornton, J. M.; Singh, J.; Price, S. L. J Mol Biol 1992, 226, 251–262.